

Combined Effects of Centrifugal and Coriolis Instability of the Flow through a Rotating Curved Duct with Rectangular Cross Section

Rabindra Nath Mondal¹, Samir Chandra Ray², Shinichiro Yanase³

¹Department of Mathematics, Jagannath University, Dhaka, Bangladesh

²Department of Mathematics, Bangabandhu Sheikh Mujibur Rahman Science and Technology University, Gopalganj, Bangladesh

³Department of Mechanical and System Engineering, Faculty of Engineering, Okayama University, Okayama, Japan

Email: rnmondal71@yahoo.com

Received 14 November 2013; revised 14 December 2013; accepted 23 December 2013

Copyright © 2014 by authors and Scientific Research Publishing Inc.

This work is licensed under the Creative Commons Attribution International License (CC BY).

<http://creativecommons.org/licenses/by/4.0/>



Open Access

Abstract

Combined effects of centrifugal and coriolis instability of the flow through a rotating curved duct with rectangular cross section have been studied numerically by using a spectral method, and covering a wide range of the Taylor number $0 \leq Tr \leq 2500$ for a constant Dean number $Dn = 2000$. The rotation of the duct about the center of curvature is imposed in the positive direction, and the effects of rotation (*Coriolis force*) on the flow characteristics are investigated. As a result, multiple branches of asymmetric steady solutions with two-, three- and multi-vortex solutions are obtained. To investigate the non-linear behavior of the unsteady solutions, time evolution calculations as well as power spectrum of the unsteady solutions are performed, and it is found that the unsteady flow undergoes through various flow instabilities in the scenario "*chaotic* → *multi-periodic* → *periodic* → *steady-state*", if Tr is increased in the positive direction. The present results show the characteristics of both the secondary flow and axial flow distribution in the flow.

Keywords

Rotating Curved Duct; Dean Number; Taylor Number; Secondary Flow; Periodic Solution

1. Introduction

Recently, great attention has been paid for the study of flows and heat transfer through rotating curved ducts and channels because of its practical application in chemical, mechanical, bio-mechanical and biological engineering. A quantitative analogy between flows in stationary curved pipes and orthogonally rotating straight pipes has been reported by Ishigaki [1] [2]. Taking this analogy as a basis, this study describes the characteristics of more general and complicated flow in rotating curved ducts. Such rotating flow passages are used in cooling systems in rotating machinery such as in gas turbines, turbo-machinery, electric generators and electric motors. The readers can refer to Berger *et al.* [3] and Nandakumar and Masliyah [4] for some outstanding reviews on curved duct flows.

One of the interesting phenomena of the flow through a curved duct is the bifurcation of the flow because generally there exist many steady solutions due to channel curvature. An early complete bifurcation study of two-dimensional (2-D) flow through a curved duct with square cross section was performed by Winters [5]. However, an extensive treatment of the flow through a curved square duct was reported by Mondal *et al.* [6]. He found a close relationship between the unsteady solutions and the bifurcation diagram of steady solutions. Ishigaki [2] examined the flow structure and friction factor numerically for both the counter-rotating and co-rotating curved circular pipe with a small curvature. Selmi *et al.* [7] examined the combined effects of system rotation and curvature on the bifurcation structure of two-dimensional flows in a rotating curved square duct. Selmi and Nandakumar [8] performed studies on the flow in rotating curved rectangular ducts. Yamamoto *et al.* [9] employed spectral method to examine the flow structure and the flow rate ratio in a rotating curved square duct flow and found six-cell phenomenon of the secondary flow. Recently, Mondal *et al.* [10] performed a comprehensive numerical study on the bifurcation structure and the stability of solutions for laminar forced convection in a rotating curved duct of square cross section, and revealed some new features on fluid flow. However, the complete flow structures under the combined action of Coriolis and centrifugal instability are still unrevealed for the rotating curved rectangular duct flow at high rotation. It is an attempt of the present study.

It is well known that, fluid flowing in a rotating curved duct is subjected to two forces: the *Coriolis force*, caused by the rotation of the duct, and *centrifugal force* caused by the curvature of the duct. These two forces affect each other, as a result complex behavior of the secondary flow and the axial flow can be obtained (Wang and Cheng [11]). For isothermal flows of a constant property fluid, however, the Coriolis force tends to produce vorticity while centrifugal force is purely hydrostatic (Zhang *et al.* [12]). When a temperature induced variation of fluid density occurs for non-isothermal flows, both Coriolis and centrifugal type buoyancy forces can contribute to the generation of vorticity (Mondal *et al.*, [13]). These two effects of rotation either enhance or counteract each other in a non-linear manner depending on the direction of wall heat flux and the flow domain. Therefore, the effect of rotation of the system is more subtle and complicated and yields new; richer features of flow and heat transfer in general, bifurcation and stability in particular, for non-isothermal flows. Mondal *et al.* [13] performed numerical prediction of the non-isothermal flows through a rotating curved square duct and revealed some of such new features. Very recently, Mondal *et al.* [14] investigated the combined effects of the Coriolis force and the centrifugal force on the flows in a rotating curved square duct numerically. The secondary flow characteristics in a curved square duct were investigated experimentally by using visualization method by Yamamoto *et al.* [15]. Three-dimensional incompressible viscous flow and heat transfer in a rotating U-shaped square duct were studied numerically by Nobari *et al.* [16]. However, there is no known study on bifurcation and unsteady flow characteristics in a rotating curved rectangular duct with large rotational speed. The present paper is, therefore, an attempt to fill up this gap.

Time dependent analysis of fully developed curved duct flows was first initiated by Yanase and Nishiyama [17] for a rectangular cross section. In that study, they investigated unsteady solutions for the case where dual solutions exist. However, time-dependent behavior of the flow in a curved rectangular duct over a wide range of aspect ratios was investigated, in detail, by Yanase *et al.* [18] numerically. They observed that periodic oscillations are available with symmetry condition while aperiodic time evolutions without symmetric condition. Wang and Yang [19] [20] performed numerical as well as experimental investigation on fully developed periodic oscillation in a curved square duct. Flow visualization in the range of Dean numbers from 50 to 500 was carried out in their experiment. They showed, both experimentally and numerically, that the temporal oscillation takes place between symmetric/asymmetric 2-cell and 4-cell flows where there are no stable steady flows. Applying spectral method, Yanase *et al.* [21] performed comprehensive numerical study of the time-dependent solutions

for the non-isothermal flows through a curved rectangular duct, and studied the effects of secondary flows on convective heat transfer. In order to study the time-dependent behavior of the unsteady solutions, recently, Mondal *et al.* [22] performed numerical prediction of the unsteady solutions through curved square duct for isothermal flow. They showed that periodic solutions turn into chaotic solution through a multi-periodic solution, if the Dean number is increased no matter what the curvature is. However, transient behavior of the unsteady solutions, such as periodic, multi-periodic or chaotic solutions, is yet unresolved for the flow through a rotating curved rectangular duct at large pressure gradient with large rotational speed. This motivated the present study to investigate the non-linear behavior of the unsteady solutions by time-evolution calculation.

In the present study, a comprehensive numerical result is presented for fully developed bifurcation structure of two-dimensional (2D) viscous incompressible fluid flow through a rotating curved rectangular duct. Flow characteristics are investigated over a wide range of Taylor number $0 \leq Tr \leq 2500$ for the Dean number $Dn = 2000$. Studying the effects of rotation on the flow characteristics, caused by the combined action of centrifugal force and Coriolis force, is an important objective of the present study.

2. Governing Equations

Consider that the flow is viscous and incompressible which is streaming through a rotating curved duct with rectangular cross section. Let $2h$ and $2l$ be the height and the width of the cross section. **Figure 1** shows the coordinate system, where C is the center of the duct crosssection and L is the radius of curvature of the duct. The x' and y' axes are taken to be in the horizontal and vertical directions respectively, and z' is the coordinate along the center-line of the duct, *i.e.*, the axial direction. The system rotates at a constant angular velocity Ω_T around the y' axis. It is assumed that the flow is uniform in the axial direction, and that it is driven by a

constant pressure gradient $G \left(G = -\frac{\partial P'}{\partial z'} \right)$ along the center-line of the duct, *i.e.* the main flow direction. Then

the continuity equation and the Navier-Stokes equation, in terms of dimensional variables, are expressed as

Continuity equation

$$\frac{\partial u'}{\partial r'} + \frac{\partial v'}{\partial y'} + \frac{u'}{r'} = 0 \quad (1)$$

Momentum equations

$$\frac{\partial u'}{\partial t'} + u' \frac{\partial u'}{\partial r'} + v' \frac{\partial u'}{\partial y'} - \frac{w'^2}{r'} - 2\Omega_T w' = -\frac{1}{\rho} \frac{\partial P'}{\partial r'} + \nu \left[\frac{\partial^2 u'}{\partial r'^2} + \frac{\partial^2 u'}{\partial y'^2} + \frac{1}{r'} \frac{\partial u'}{\partial r'} - \frac{u'}{r'^2} \right], \quad (2)$$

$$\frac{\partial v'}{\partial t'} + u' \frac{\partial v'}{\partial r'} + v' \frac{\partial v'}{\partial y'} = -\frac{1}{\rho} \frac{\partial P'}{\partial y'} + \nu \left[\frac{\partial^2 v'}{\partial r'^2} + \frac{1}{r'} \frac{\partial v'}{\partial r'} + \frac{\partial^2 v'}{\partial y'^2} \right], \quad (3)$$

$$\frac{\partial w'}{\partial t'} + u' \frac{\partial w'}{\partial r'} + v' \frac{\partial w'}{\partial y'} + \frac{u' w'}{r'} + 2\Omega_T u' = -\frac{1}{\rho} \frac{1}{r'} \frac{\partial P'}{\partial z'} + \nu \left[\frac{\partial^2 w'}{\partial r'^2} + \frac{\partial^2 w'}{\partial y'^2} + \frac{1}{r'} \frac{\partial w'}{\partial r'} - \frac{w'}{r'^2} \right], \quad (4)$$

where $r' = L + x'$, and u', v' and w' are the dimensional velocity components in the x', y' and z' directions respectively. In Equations (1) to (4) the variables with prime denote the dimensional quantities. To non-dimensionalize the equations, we use the non-dimensional variables defined as

$$u = \frac{u'}{U_0}, \quad v = \frac{v'}{U_0}, \quad w = \frac{\sqrt{2\delta}}{U_0} w', \quad x = \left(\frac{x'}{l} - \frac{1}{\delta} \right), \quad \bar{y} = \frac{y'}{l}, \quad z = \frac{z'}{l}, \quad t = \frac{U_0}{l} t', \quad \delta = \frac{l}{L}, \quad P = \frac{P'}{\rho U_0^2},$$

where u, v and w are the non-dimensional velocity components in the x, y and z directions, respectively; t is the non-dimensional time, P is the non-dimensional pressure, δ is the non-dimensional curvature defined as

$\delta = \frac{l}{L}$. The sectional stream function ψ is introduced as

$$u = \frac{1}{1+\delta x} \frac{\partial \psi}{\partial y}, \quad v = -\frac{1}{1+\delta x} \frac{\partial \psi}{\partial x}. \quad (5)$$

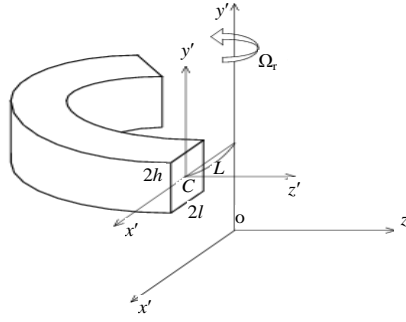


Figure 1. Rotating coordinate system.

Then, the basic equations for w and ψ are expressed in terms of non-dimensional variables as

$$(1 + \delta x) \frac{\partial w}{\partial t} + \frac{1}{a} \frac{\partial(w, \psi)}{\partial(x, y)} - Dn + \frac{\delta^2 w}{1 + \delta x} = (1 + \delta x) \Delta_2 w - \frac{\delta}{a(1 + \delta x)} \frac{\partial \psi}{\partial y} w + \delta \frac{\partial w}{\partial x} - \delta Tr \frac{\partial \psi}{\partial y}, \quad (6)$$

$$\left(\Delta_2 - \frac{\delta}{1 + \delta x} \frac{\partial}{\partial x} \right) \frac{\partial \psi}{\partial t} = -\frac{1}{a(1 + \delta x)} \frac{\partial(\Delta_2 \psi, \psi)}{\partial(x, y)} + \frac{\delta}{a(1 + \delta x)^2} \left[\frac{\partial \psi}{\partial y} \left(2\Delta_2 \psi - \frac{3\delta}{1 + \delta x} \frac{\partial \psi}{\partial x} + \frac{\partial^2 \psi}{\partial x^2} \right) - \frac{\partial \psi}{\partial x} \frac{\partial^2 \psi}{\partial x \partial y} \right] + \frac{\delta}{(1 + \delta x)^2} \times \left[3\delta \frac{\partial^2 \psi}{\partial x^2} - \frac{3\delta^2}{1 + \delta x} \frac{\partial \psi}{\partial x} \right] - \frac{2\delta}{1 + \delta x} \frac{\partial}{\partial x} \Delta_2 \psi + \frac{1}{a} w \frac{\partial w}{\partial y} + \Delta_2^2 \psi + \frac{1}{2} Tr \frac{\partial w}{\partial y}, \quad (7)$$

where,

$$\Delta_2 \equiv \frac{\partial^2}{\partial x^2} + \frac{1}{a^2} \frac{\partial^2}{\partial y^2}, \quad \frac{\partial(f, g)}{\partial(x, y)} \equiv \frac{\partial f}{\partial x} \frac{\partial g}{\partial y} - \frac{\partial f}{\partial y} \frac{\partial g}{\partial x}. \quad (8)$$

The non-dimensional parameters Dn , the Dean number and Tr , the Taylor number which appear in Equations (6) and (7) are defined as:

$$Dn = \frac{Gl^3}{\mu\nu} \sqrt{\frac{2l}{L}}, \quad Tr = \frac{2\sqrt{2}\delta\Omega_r l^3}{\nu\delta} \quad (9)$$

In the present study, Tr varies while Dn , δ , a and Pr are fixed as $Dn = 2000$, $\delta = 0.1$, $a = 1.5$ and $Pr = 7.0$ (water). The rigid boundary conditions for w and ψ are used as

$$w(\pm 1, y) = w(x, \pm 1) = \psi(\pm 1, y) = \psi(x, \pm 1) = \frac{\partial \psi}{\partial x}(\pm 1, y) = \frac{\partial \psi}{\partial y}(x, \pm 1) = 0 \quad (10)$$

3. Numerical Calculations

In order to solve Equations (6) to (7) numerically, the spectral method is used (Gottlieb and Orazag [23]). By this method the variables are expanded by using the expansion functions $\phi_n(x)$ and $\psi_n(x)$ as

$$\left. \begin{aligned} \phi_n(x) &= (1 - x^2) C_n(x), \\ \psi_n(x) &= (1 - x^2)^2 C_n(x) \end{aligned} \right\} \quad (11)$$

where $C_n(x) = \cos(n \cos^{-1}(x))$ is the n^{th} order Chebyshev polynomial. $w(x, y, t)$ and $\psi(x, y, t)$ are expanded in terms of the expansion functions $\phi_n(x)$ and $\psi_n(x)$ as

$$\left. \begin{aligned} w(x, y, t) &= \sum_{m=0}^M \sum_{n=0}^N w_{mn}(t) \phi_m(x) \phi_n(y), \\ \psi(x, y, t) &= \sum_{m=0}^M \sum_{n=0}^N \psi_{mn}(t) \psi_m(x) \psi_n(y). \end{aligned} \right\} \quad (12)$$

First, steady solutions are obtained by the Newton-Rapshon iteration method. Then, in order to calculate the unsteady solutions, the Crank-Nicolson and Adams-Bash-forth methods together with the function expansion (12) and the collocation methods are applied.

4. Flux through the Duct

The dimensional total flux Q' through the duct in the rotating coordinate system is calculated by:

$$Q' = \int_{-h}^h \int_{-l}^l w' dx' dy' = v d Q, \quad (13)$$

where

$$Q = \int_{-1}^1 \int_{-1}^1 w dx dy \quad (14)$$

is the dimensionless total flux. The mean axial velocity, \bar{w}' is expressed as $\bar{w}' = \frac{Qv}{4l}$. In the present study, Q is used to denote the steady solution branches and to pursue time evolution of the unsteady solutions.

5. Results and Discussion

5.1. Steady Solutions and Flow Patterns

We obtained four branches of symmetric/asymmetric steady solutions for the Dean number $Dn = 2000$ over the Taylor number $0 \leq Tr \leq 2500$, as shown in **Figure 2**. The four steady solution branches are named the *first steady solution branch* (first branch, thick solid line), the *second steady solution branch* (second branch, thin solid line), the *third steady solution branch* (third branch, thick dotted line) and the *fourth steady solution branch* (fourth branch, long dash line), respectively. The steady solution branches are obtained by the path continuation technique (Keller [24]) with various initial guesses as discussed by Mondal [25]. In this regard, it should be noted that Mondal *et al.* [13] also obtained four branches of steady solutions for the non-isothermal flow through a rotating curved square duct.

Then, we obtained secondary vortices on various branches of steady solutions, and it is found that at the same value of Tr sometimes we obtain two-vortex solution, while sometimes two- and multi-vortex solutions. It is found that the first and fourth steady solution branches consist of symmetric solutions while the second and third branches consist of asymmetric solutions. The first branch consists of symmetric two-, four-, six-, eight- and ten-vortex solutions, the second branch is composed of asymmetric two- and four-vortex solutions, the third branch is characterized by asymmetric two- and four-vortex solutions, while the fourth branch is comprised with asymmetric two- to ten-vortex solutions. These vortices are generated due to the combined action of the *centrifugal force* and *Coriolis force*. The steady solution branches as well as the formation of secondary vortices on various branches are not shown here for brevity; however, we show some contours of secondary flow patterns and axial flow distribution at some specific values of Tr . To observe the pattern variation and development of the *secondary vortices*, also called the *Dean vortices*, contours of secondary flow patterns are shown in **Figure 3** at various values of Tr for $Dn = 2000$. In the figures of the secondary flow, solid lines ($\psi \geq 0$) show that the secondary flow is in the counter clockwise direction while the dotted lines ($\psi < 0$) in the clockwise direction. As seen in **Figure 3**, the secondary flow is two-, four-, six-, eight- and ten-vortex solutions, which are obtained on different branches of steady solutions. **Figure 4** shows typical contours of secondary flow patterns and axial flow distribution on the steady solution branch at $Tr = 600$, where it is found that the secondary flow consists of symmetric and asymmetric two- to ten-vortex solutions at $Tr = 600$.

5.2. Unsteady Solutions

In order to investigate the non-linear behavior of the unsteady solutions, time-evolution calculations of the unsteady solutions are performed for $Dn = 2000$ over the Taylor number $0 \leq Tr \leq 2500$. Time evolution of Q for $Tr \geq 2030$ shows that the value of Q quickly approaches steady-state solution no matter what the initial condition we use. Then, in order to see the unsteady flow characteristics for $Tr < 2030$ and $Tr > 2030$, time

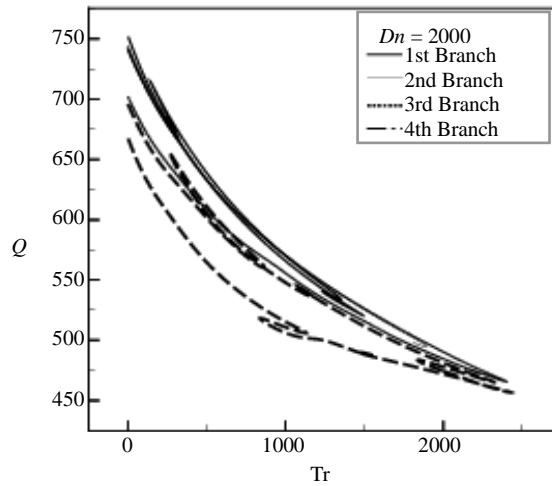


Figure 2. Solution structure of the steady solutions for $0 \leq Tr \leq 2500$ at $Dn = 2000$.

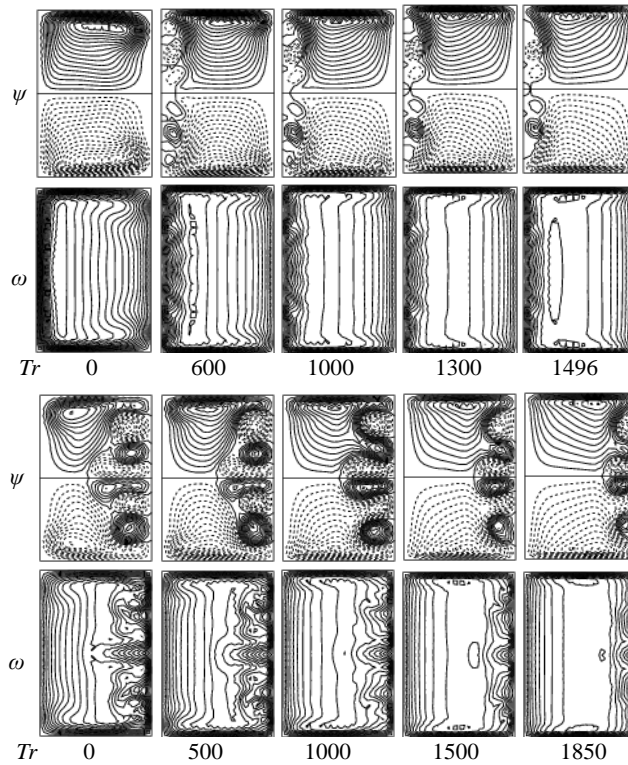


Figure 3. Streamlines of secondary flow (top) and axial flow (bottom) on the steady solution branches at various values of Tr .

evolutions of Q are then performed for $Tr = 0, 500, 1000, 1500, 1870, 1880, 1900, 1950$ and 2050 . **Figure 5(a)** shows time-evolution of Q for $Tr = 0$ at $Dn = 2000$, where it is seen that the flow oscillates irregularly, *i.e.* the flow is chaotic. This chaotic oscillation is well justified by drawing the power spectrum as shown in **Figure 5(b)**, where it is seen that lots of continuous line spectra with different frequencies are available, which suggests that the unsteady flow at $Tr = 0$ is chaotic. Typical contours of secondary flow patterns and axial flow distribution at $Tr = 0$ are shown in **Figure 5(c)**, where it is seen that the flow oscillates between asymmetric six- to eight-vortex solutions. Time-evolution of Q for $Tr = 500$ is shown in **Figure 6(a)**, where it is seen that the

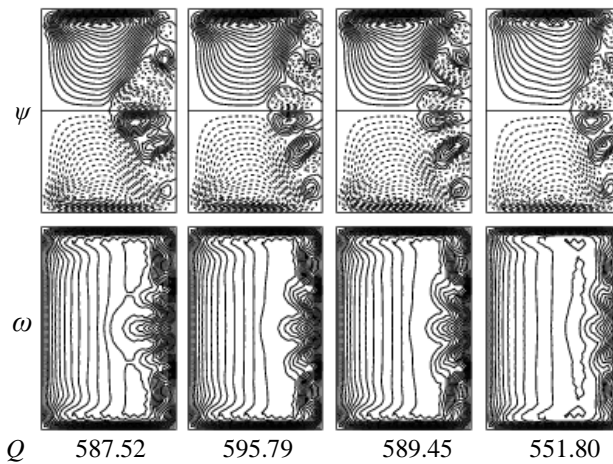


Figure 4. Streamlines of secondary flow (top) and axial flow (bottom) on the fourth steady solution branch for various values of Q at $Tr = 600$

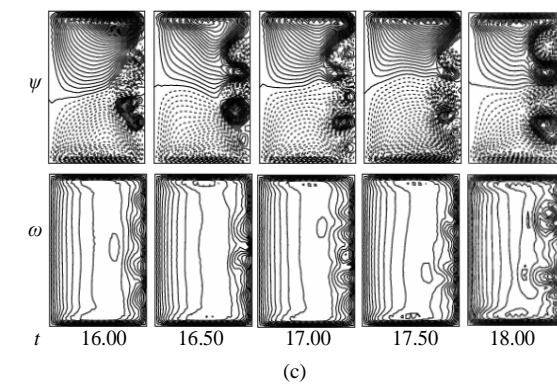
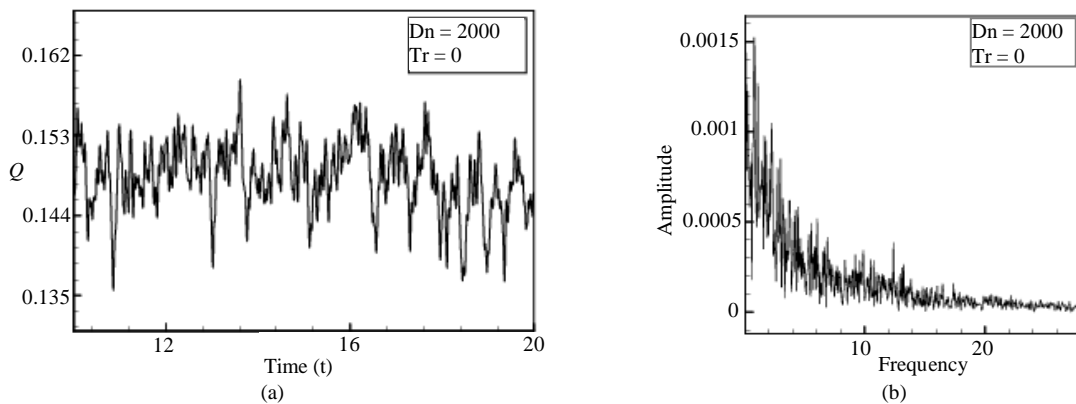


Figure 5. (a) Time evolution of Q for $Dn = 2000$ and $Tr = 0$; (b) Power spectrum for $Tr = 0$; (c) Streamlines of secondary flow (top) and axial flow for $Tr = 0$.

flow is also chaotic. Power spectrum of the time change of Q for $Tr = 500$ is shown in **Figure 6(b)**, which justifies the chaotic behavior of the unsteady solution at $Tr = 500$. Typical contours of secondary flow patterns and axial flow distribution for $Tr = 500$ are shown in **Figure 6(c)**, where it is seen that the flow oscillates between asymmetric six- to eight-vortex solutions.

Then we performed time-evolutions of Q for $Tr = 1000$ and 2000 . The results are shown in **Figures 7(a)** and **8(a)** respectively. It is found that the unsteady flow further oscillates irregularly, *i.e.* chaotic. In order to see the mode of the chaotic oscillations, we then performed power spectra of the time change of Q as shown in

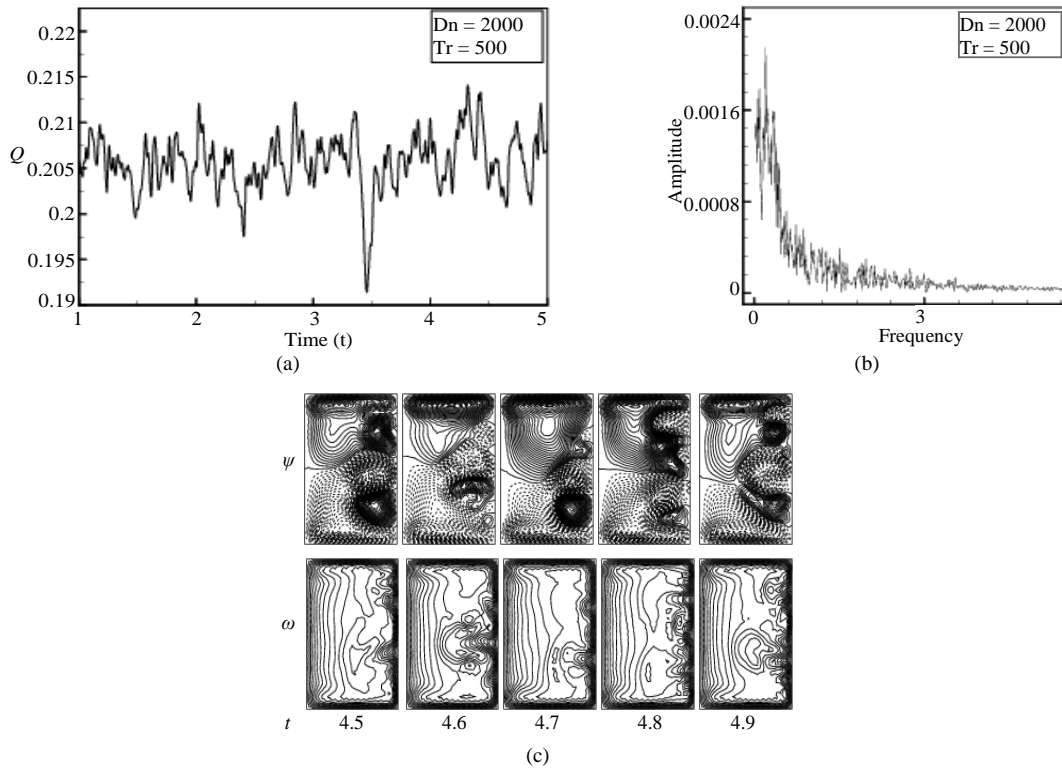


Figure 6. (a) Time evolution of Q for $Dn = 2000$ and $Tr = 500$; (b) Power spectrum for $Tr = 500$; (c) Streamlines of secondary flow (top) and axial flow (bottom) for $Tr = 500$.

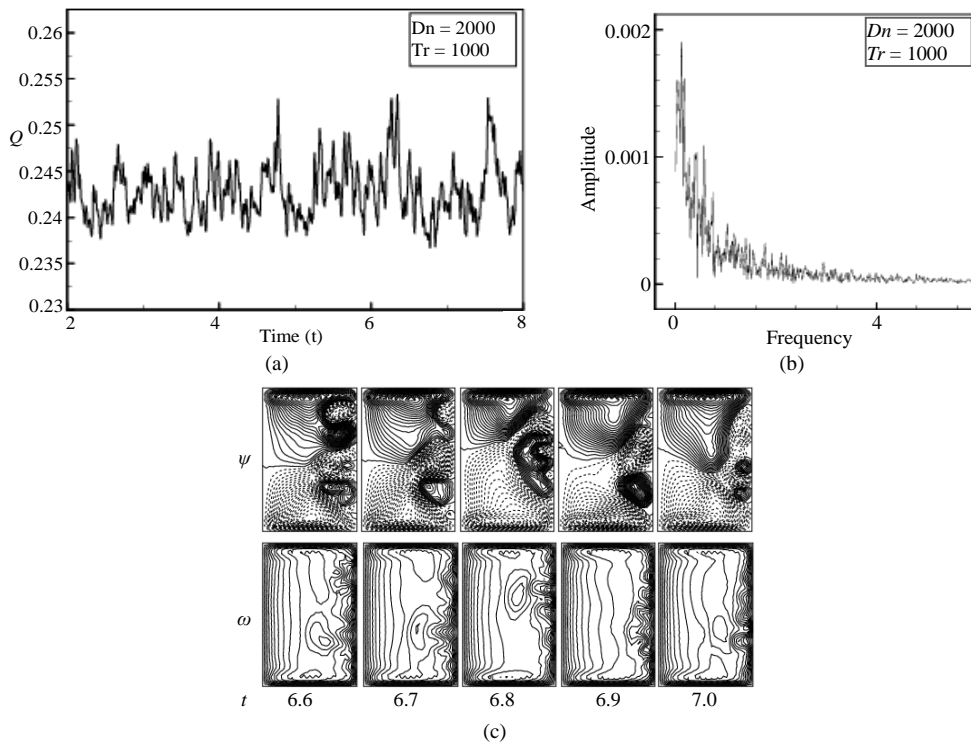


Figure 7. (a) Time evolution of Q for $Dn = 2000$ and $Tr = 1000$; (b) Power spectrum of Q for $Tr = 1000$; (c) Streamlines of secondary flow (top) and axial flow (bottom) for $Tr = 1000$.

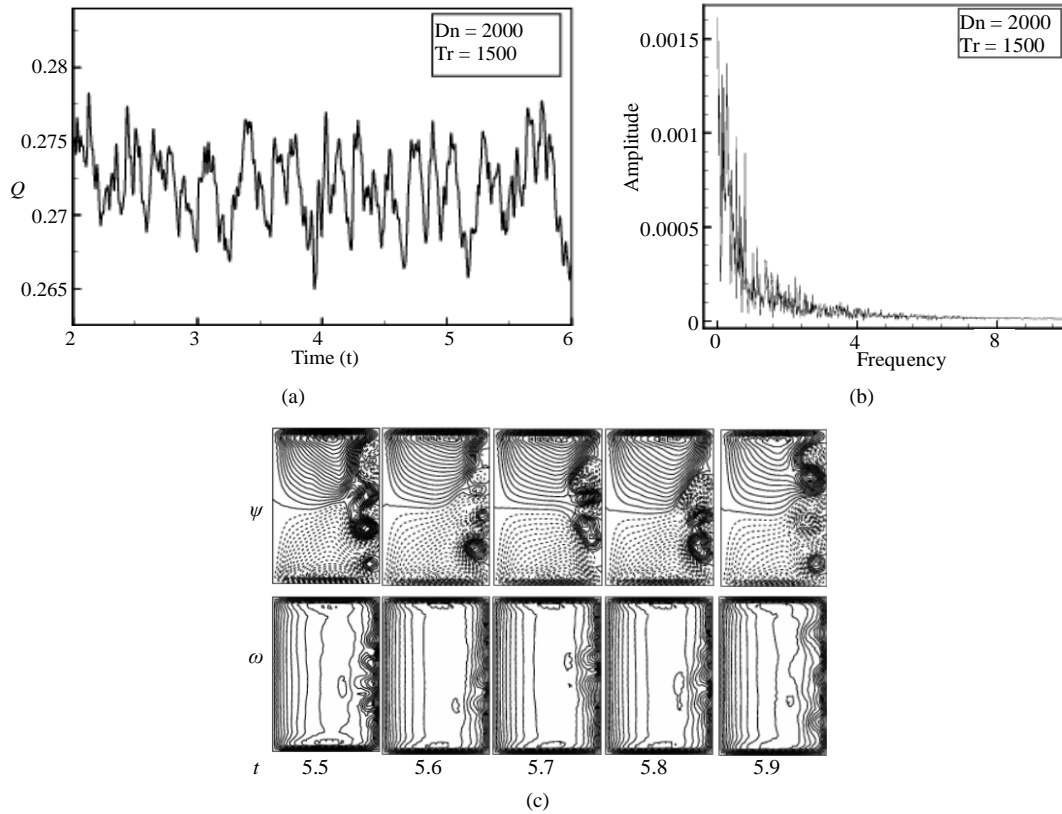


Figure 8. (a) Time evolution of Q for $Dn = 2000$ and $Tr = 1500$; (b) Power spectrum for $Tr = 1500$; (c) Streamlines of secondary flow (top) and axial flow (bottom) for $Tr = 1500$.

Figures 7(b) and **8(b)** for $Tr = 1000$ and $Tr = 1500$ respectively, where lots of continuous line spectra with different frequencies are seen, which suggests that the unsteady flow at $Tr = 1000$ and $Tr = 1500$ are chaotic. Typical contours of secondary flow patterns and axial flow distribution for $Tr = 1000$ and $Tr = 1500$ are shown in **Figures 7(c)** and **8(c)** respectively, where it is seen that the flow oscillates between asymmetric four- to ten-vortex solutions. **Figure 9(a)** shows time-evolution of Q for $Tr = 1870$, where it is seen that the flow is chaotic. This chaotic solution is well justified by the power spectrum of the time change of Q as shown in **Figure 9(b)**, where it is seen that lots of continuous line spectra with different frequencies are available, which suggests that the flow is chaotic. Secondary flow patterns and axial flow distribution for $Tr = 1870$ are shown in **Figure 9(c)**, where it is seen that the flow oscillates between asymmetric six- and eight-vortex solutions.

Then we performed time evolution of Q for $Tr = 1880$ as shown in **Figure 10(a)**. As seen in **Figure 10(a)**, the time-dependent solution for $Tr = 1880$ is multi-periodic. Power spectrum of the time change of Q for $Tr = 1880$ is also shown in **Figure 10(b)**, in which not only the line spectrum of the fundamental frequency and its harmonics but also other line spectrum and their harmonics are seen, which suggests that the flow is multi-periodic. Secondary flow patterns and axial flow distributions are shown in **Figure 10(c)**, for one period of oscillation at $5.7 \leq t \leq 5.91$ where it is seen that the unsteady flow at $Tr = 1880$ oscillates between asymmetric four- and six-vortex solutions.

Next, time evolution of Q for $Tr = 1900$ is shown in **Figure 11(a)**, where it is seen that the flow oscillates periodically. It is justified by the power spectrum as shown in **Figure 11(b)**, where the fundamental frequency and its harmonics as well as line spectra with small frequency is seen, which indicates that the oscillation presented in **Figure 11(b)** is multi-periodic, but not periodic. It is seen that the fundamental mode is higher than that of the other modes, which clearly suggests that the flow at $Tr = 1900$ is perfectly multi-periodic. Contours of secondary flow patterns and axial flow distributions are shown in **Figure 11(c)**. As seen in **Figure 11(c)**, the unsteady solution at $Tr = 1900$ oscillates in the asymmetric six-vortex solutions. Then, we investigated time-dependent solution of Q for $Tr = 1950$ at $Dn = 2000$ as shown in **Figure 12(a)**. It is found that the flow

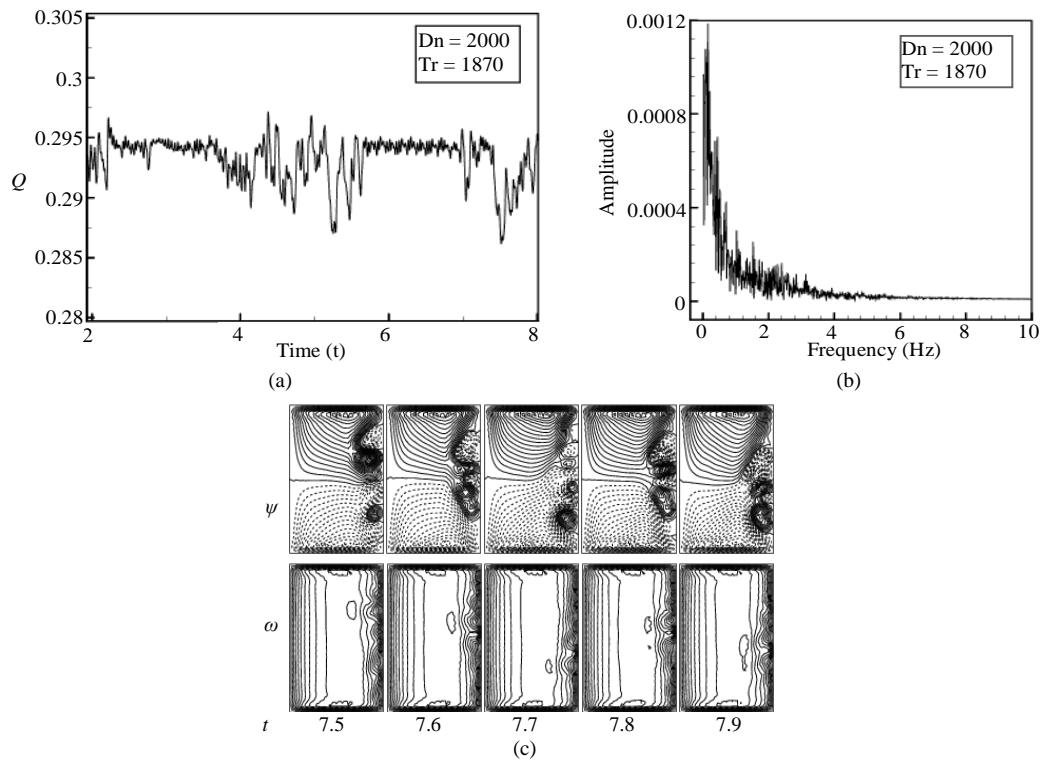


Figure 9. (a) Time evolution of Q for $Dn = 2000$ and $Tr = 1870$; (b) Power spectrum for $Tr = 1870$; (c) Streamlines of secondary flow (top) and axial flow (bottom) for $Tr = 1870$.

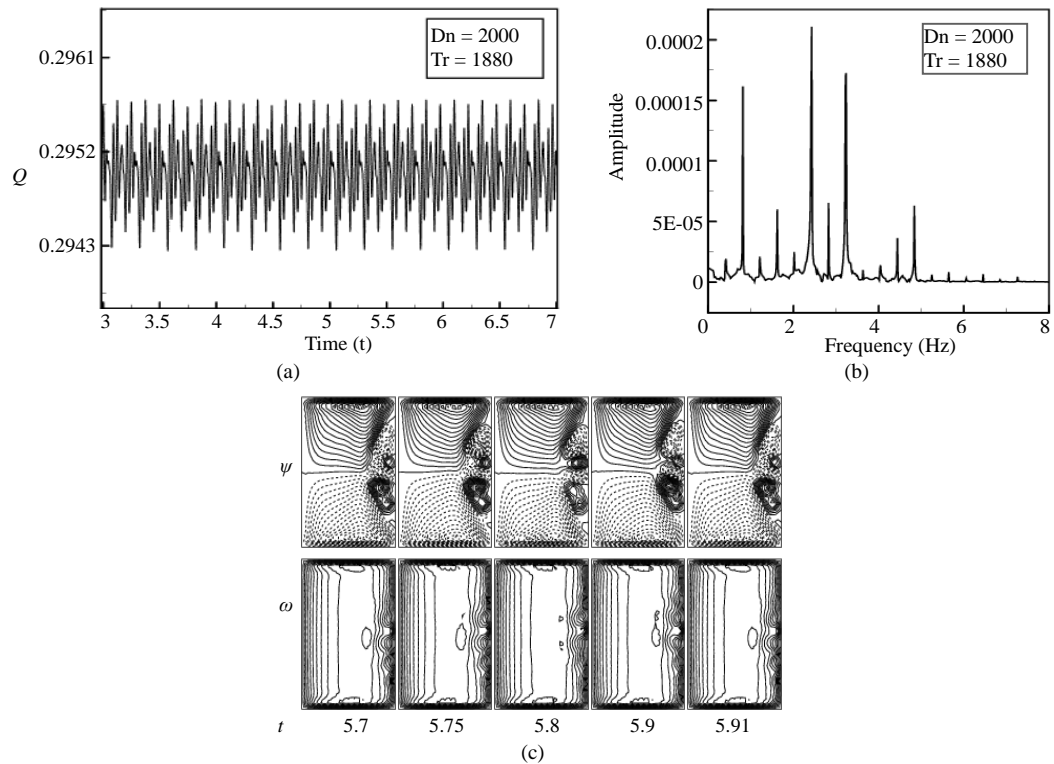


Figure 10. (a) Time evolution of Q for $Tr = 1880$ at $Dn = 2000$; (b) Power spectrum for $Tr = 1880$; (c) Streamlines of secondary flow (top) and axial flow (bottom) for $Tr = 1880$.

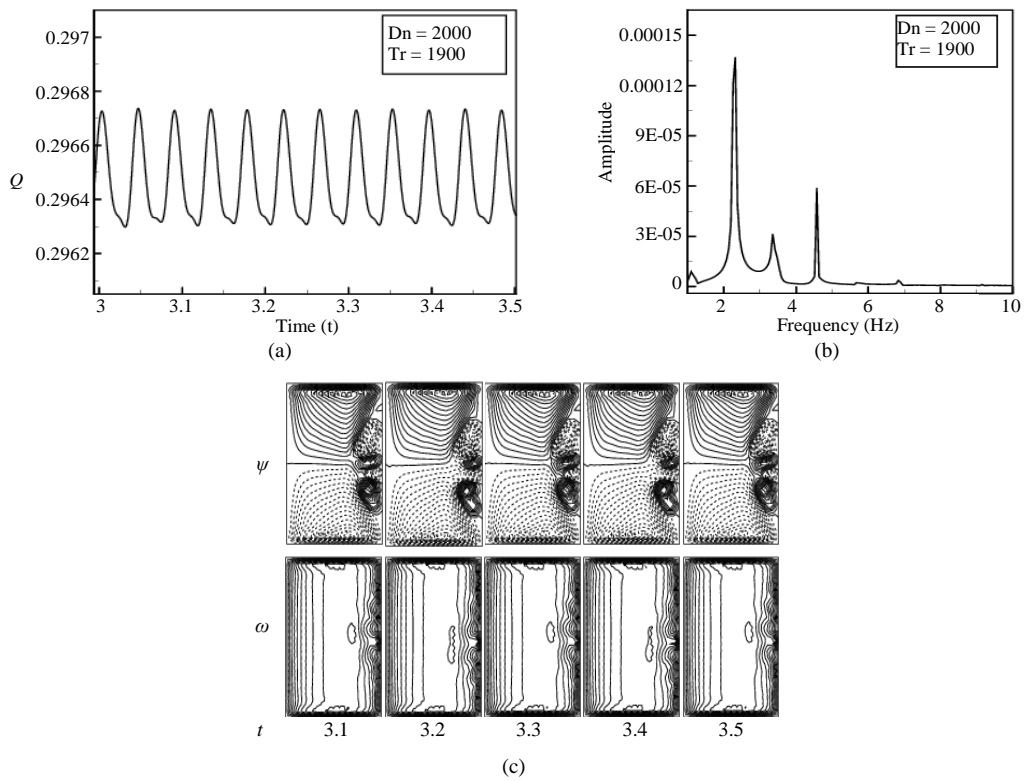


Figure 11. (a) Time evolution of Q for $Tr = 1900$ and $Dn = 2000$; (b) Power spectrum for $Tr = 1900$; (c) Streamlines of secondary flow (top) and axial flow (bottom) for $Tr = 1900$.

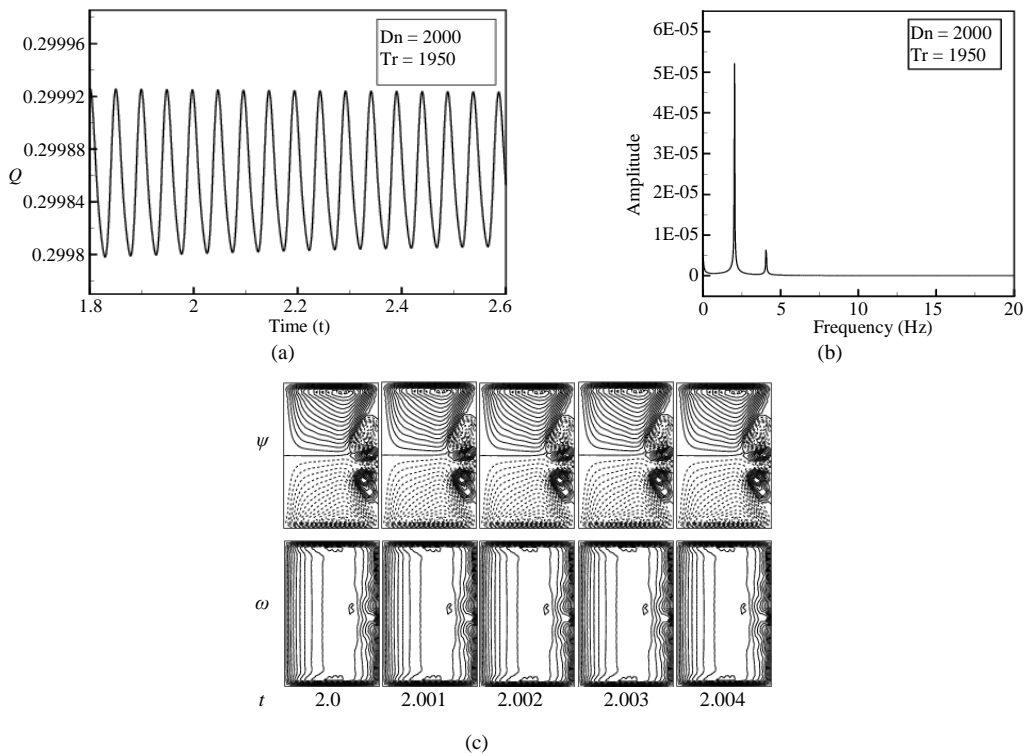


Figure 12. (a) Time evolution of Q for $Tr = 1950$ at $Dn = 2000$; (b) Power spectrum for $Tr = 1950$; (c) Streamlines of secondary flow (top) and axial flow (bottom) for $Tr = 1950$.

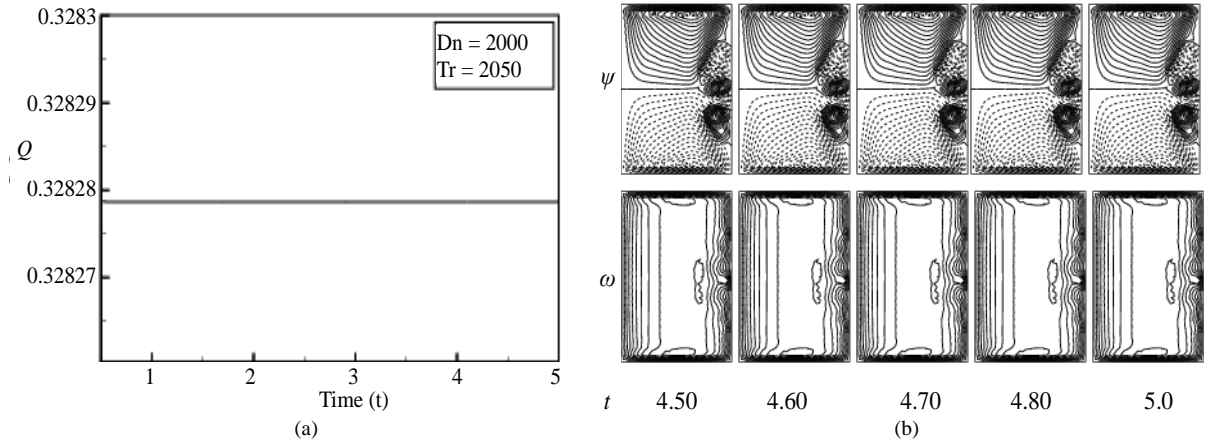


Figure 13. (a) Time evolution of Q for $Dn = 2000$ and $Tr = 2050$; (b) Streamlines of secondary flow (top) and axial flow (bottom) for $Tr = 2050$.

oscillates periodically, which is well justified by the power spectrum of the time evolution of Q as shown in **Figure 12(b)**, where only the line spectrum of the fundamental frequency and its harmonics are seen, which suggests that the flow is purely periodic at $Tr = 1950$.

Secondary flow patterns and axial flow distribution for $Tr = 1950$ are then shown in **Figure 12(c)**, where it is seen that the flow at $Tr = 1950$ oscillates in the asymmetric six-vortex solutions. **Figure 13(a)** shows time evolution of Q for $Tr = 2050$ at $Dn = 2000$. It is found that the flow does not oscillate but goes steady-state, so that the unsteady solution at $Tr = 2050$ is a steady-state solution. Typical contours of secondary flow patterns and axial flow distribution for $Tr = 2050$ are also shown in **Figure 13(b)**, where it is seen that the unsteady flow at $Tr = 2050$ is an asymmetric six-vortex solution. It is noticed that axial flow is shifted near the outer wall of the duct as the rotational speed increases.

6. Conclusions

A numerical study on the fully developed two-dimensional flow of viscous incompressible fluid through a rotating curved rectangular duct of aspect ratio 1.5 and curvature 0.1 has been performed by using the spectral method, and covering a wide range of the Taylor number $0 \leq Tr \leq 2500$ for the Dean number $Dn = 2000$. We investigated flow characteristics for positive rotation of the duct, and obtained secondary flow patterns and axial flow distribution for several values of Tr .

We obtained four branches of symmetric and asymmetric steady solutions with two- and multi-vortex solutions on various branches. The first branch consists of symmetric two-, four- and multi-vortex solutions. The second branch is composed of asymmetric two-, three- and four-vortex solutions; the third steady solution branch is composed of asymmetric two-, three- and four-vortex solutions, while the fourth steady solution branch symmetric six-, eight- and ten-vortex solutions. Then, In order to study the non-linear behavior of the unsteady solutions, time-evolution calculations as well as power spectrum of the unsteady solutions are performed, and it is found that the chaotic flow turns into steady-state flow through periodic flow in the scenario “*chaotic* \rightarrow *multi-periodic* \rightarrow *periodic* \rightarrow *steady-state*”, if Tr is increased from zero. It is found that at no rotation, the flow is chaotic but as the rotational speed increases, the chaotic flow turns into steady-state flow through multi-periodic and periodic oscillations. The reason is that combined effect of centrifugal and Coriolis force counteract each other in a nonlinear manner which results in chaotic flow to turn into steady-state flow. Performing the power spectrum of the solutions was found to be fruitful for the investigation of unsteady flow behavior more accurately. Maximum axial flow was found to be shifted near the outer wall of the duct as the rotational speed increases.

Acknowledgements

Shinichiro Yanase, one of the authors, expresses his cordial thanks to the Japan Ministry of Education, Culture,

Sports, Science and Technology for the financial support through the Grant-in-Aid for Scientific Research, No. 24560196.

References

- [1] Ishigaki, H. (1993) Fundamental Characteristics of Laminar Flows in a Rotating Curved Pipe. *Transactions of JSME*, **59**, 1494-1501.
- [2] Ishigaki, H. (1996) Laminar Flow in Rotating Curved Pipes. *Journal of Fluid Mechanics*, **329**, 373-388. <http://dx.doi.org/10.1017/S0022112096008956>
- [3] Berger, S.A., Talbot, L. and Yao, L.S. (1983) Flow in Curved Pipes. *Annual Review of Fluid Mechanics*, **35**, 461-512. <http://dx.doi.org/10.1146/annurev.fl.15.010183.002333>
- [4] Nandakumar, K. and Masliyah, J.H. (1986) Swirling Flow and Heat Transfer in Coiled and Twisted Pipes. *Advanced Transport Processes*, **4**, 49-112.
- [5] Winters, K.H. (1987) A Bifurcation Study of Laminar Flow in a Curved Tube of Rectangular Cross-Section. *Journal of Fluid Mechanics*, **180**, 343-369. <http://dx.doi.org/10.1017/S0022112087001848>
- [6] Mondal, R.N., Kaga, Y., Hyakutake, T. and Yanase, S. (2007) Bifurcation Diagram for Two-Dimensional Steady Flow and Unsteady Solutions in a Curved Square Duct. *Fluid Dynamics Research*, **39**, 413-446. <http://dx.doi.org/10.1016/j.fluidyn.2006.10.001>
- [7] Selmi, M., Nandakumar, K. and Finlay, W.H. (1994) A Bifurcation Study of Viscous Flow through a Rotating Curved Duct. *Journal of Fluid Mechanics*, **262**, 353-375. <http://dx.doi.org/10.1017/S0022112094000534>
- [8] Selmi, M. and Nandakumar, K. (1999) Bifurcation Study of the Flow through Rotating Curved Ducts. *Physics of Fluids*, **11**, 2030-2043. <http://dx.doi.org/10.1063/1.870066>
- [9] Yamamoto, K., Yanase, S. and Alam, M.M. (1999) Flow through a Rotating Curved Duct with Square Cross-Section. *Journal of the Physical Society of Japan*, **68**, 1173-1184. <http://dx.doi.org/10.1143/JPSJ.68.1173>
- [10] Mondal, R.N., Islam, M.R., Uddin, M.S. and Datta, A.K. (2010) Flow through a Rotating Curved Square Duct: The Case of Positive Rotation. *Journal of Physical Science*, **14**, 145-163.
- [11] Wang, L.Q. and Cheng, K.C. (1996) Flow Transitions and Combined Free and Forced Convective Heat Transfer in Rotating Curved Channels: The Case of Positive Rotation. *Physics of Fluids*, **8**, 1553-1573. <http://dx.doi.org/10.1063/1.868930>
- [12] Zhang, J.S., Zhang, B.Z. and Jü, J. (2001) Fluid Flow in a Rotating Curved Rectangular Duct. *International Journal of Heat and Fluid Flow*, **22**, 583-592. [http://dx.doi.org/10.1016/S0142-727X\(01\)00126-6](http://dx.doi.org/10.1016/S0142-727X(01)00126-6)
- [13] Mondal, R.N., Alam, M.M. and Yanase, S. (2007) Numerical Prediction of Non-Isothermal Flows through a Rotating Curved Duct with Square Cross Section. *Thammasat International Journal of Science and Technology*, **12**, 24-43.
- [14] Mondal, R.N., Datta, A.K. and Mondal, B. (2011) Bifurcation Study of Thermal Flows through a Rotating Curved Square Duct. *Bangladesh Journal of Scientific and Industrial Research*, **48**, 59-70.
- [15] Yamamoto, K., Wu, X., Nozaki, K. and Hayamizu, Y. (2006) Visualization of Taylor-Dean Flow in a Curved Duct of Square Cross-Section. *Fluid Dynamics Research*, **38**, 1-18. <http://dx.doi.org/10.1016/j.fluidyn.2005.09.002>
- [16] Nobari, M.R.H., Nousha, A. and Damangir, E. (2009) A Numerical Investigation of Flow and Heat Transfer in Rotating U-Shaped Square Ducts. *International Journal of Thermal Sciences*, **48**, 590-601. <http://dx.doi.org/10.1016/j.ijthermalsci.2008.04.001>
- [17] Yanase, S. and Nishiyama, K. (1988) On the Bifurcation of Laminar Flows through a Curved Rectangular Tube. *Journal of the Physical Society of Japan*, **57**, 3790-3795. <http://dx.doi.org/10.1143/JPSJ.57.3790>
- [18] Yanase, S., Kaga, Y. and Daikai, R. (2002) Laminar Flow through a Curved Rectangular Duct over a Wide Range of the Aspect Ratio. *Fluid Dynamics Research*, **31**, 151-183. [http://dx.doi.org/10.1016/S0169-5983\(02\)00103-X](http://dx.doi.org/10.1016/S0169-5983(02)00103-X)
- [19] Yang, T. and Wang, L. (2003) Bifurcation and Stability of Forced Convection in Rotating Curved Ducts of Square Cross Section. *International Journal of Heat and Mass Transfer*, **46**, 613-629. [http://dx.doi.org/10.1016/S0017-9310\(02\)00329-0](http://dx.doi.org/10.1016/S0017-9310(02)00329-0)
- [20] Wang, L.Q. and Yang, T.L. (2004) Multiplicity and Stability of Convection in Curved Ducts: Review and Progress. *Advances in Heat Transfer*, **38**, 203-256. [http://dx.doi.org/10.1016/S0065-2717\(04\)38004-4](http://dx.doi.org/10.1016/S0065-2717(04)38004-4)
- [21] Yanase, S., Mondal, R.N. and Kaga, Y. (2005) Numerical Study of Non-Isothermal Flow with Convective Heat Transfer in a Curved Rectangular Duct. *International Journal of Thermal Sciences*, **44**, 1047-1060. <http://dx.doi.org/10.1016/j.ijthermalsci.2005.03.013>
- [22] Mondal, R.N., Kaga, Y., Hyakutake, T. and Yanase, S. (2006) Effects of Curvature and Convective Heat Transfer in Curved Square Duct Flows. *Journal of Fluids Engineering, ASME Journals*, **128**, 1013-1023.

<http://dx.doi.org/10.1115/1.2236131>

- [23] Gottlieb, D. and Orazag, S.A. (1977) Numerical Analysis of Spectral Methods. Society for Industrial and Applied Mathematics, Philadelphia. <http://dx.doi.org/10.1137/1.9781611970425>
- [24] Keller, H.B. (1987) Lectures on Numerical Methods in Bifurcation Problems. Springer, Berlin.
- [25] Mondal, R.N. (2006) Isothermal and Non-Isothermal Flows through Curved Duct with Square and Rectangular Cross-Section. Ph.D. Thesis, Okayama University, Okayama.